

Amorphous and ordered organosilicas functionalized with amine groups as sorbents of platinum (II) ions

Mariusz Barczak · Ryszard Dobrowolski ·
Joanna Dobrzyńska · Emil Zięba · Andrzej Dąbrowski

Received: 12 November 2012 / Accepted: 5 February 2013 / Published online: 20 February 2013
© The Author(s) 2013. This article is published with open access at Springerlink.com

Abstract Two groups of amine-functionalized organosilicas have been synthesized: amorphous polysiloxane xerogels (APX) and ordered mesoporous organosilicas (OMO) by co-condensation of tetraethoxysilane and appropriate alkoxy silanes: aminopropyltriethoxysilane and *N*-[3-(trimethoxysilyl)propyl]ethylenediamine. The obtained materials were characterized by sorption measurements, X-ray diffractometry, elemental analysis, transmission electron microscopy, and scanning electron microscopy. The OMO samples have well developed porous structure—the values of specific surface area are in the range 740–840 m²/g. While the APX samples are less porous having the corresponding values in the range 280–520 m²/g. The sizes of the ordered mesopores of OMO are in the range 5.9–6.5 nm while for the APX they are 2.9–12.1 nm indicating structural differences between both groups of the samples. All samples were tested as the sorbents of Pt(II) ions. The influence of various parameters such as pH, contact time, equilibrium concentration on Pt(II) adsorption ability onto prepared adsorbents was studied in detail. Additionally, the effect of chloride concentration on Pt(II) adsorption was investigated. The values of static sorption capacities were in the range of 32–102 mg_{Pt(II)}/g and 20–139 mg_{Pt(II)}/g for OMO and APX series, respectively.

Keywords Sol–gel · Polysiloxanes · Organosilicas · Functionalization · Adsorption · Platinum

1 Introduction

The sol–gel method offers great opportunities for designing hybrid porous materials (Brinker and Scherer 1990; Kickelbick 2007; Ferey 2008). In particular porous materials based on silica are widely exploited nowadays in many fields including adsorption, catalysis, sensors, membranes (Sakka 2005; Shea et al. 2004; Collinsona 1999). The wide potentialities of the sol–gel method were demonstrated at the end of the past century by the synthesis of silicas functionalized with the groups capable of complexation (Avnir et al. 1998; Feng et al. 1997). The functional surface layer is a precise tool for affecting the properties of xerogels, for example, sorption characteristics, due to the possibilities of varying both the nature of the functional groups in such a layer and the porous structure.

Functionalized amorphous polysiloxane xerogels (APX) are a class of hybrid organic–inorganic materials, usually obtained by hydrolysis and polycondensation reactions of tetraethoxysilane (TEOS) and appropriate organosilicas monomers (Slinyakova 1988; El-Nahhala and El-Ashgarb 2007). The sol–gel method provides here a possibility to design—on a molecular level—the considered materials keeping control over their chemical and physical properties, including structure-adsorption characteristics (Loy et al. 1996; Dąbrowski et al. 2007). Particularly, this method allows for obtaining micro- and mesoporous materials with high specific surface areas. Thus, APX were tested as effective sorbents for the preconcentration, separation and extraction of heavy metal ions under static and dynamic conditions, as well as catalysts for different reactions

M. Barczak (✉) · R. Dobrowolski · J. Dobrzyńska ·
A. Dąbrowski
Faculty of Chemistry, Maria Curie-Skłodowska University,
Maria Curie-Skłodowska Sq. 3, 20-031 Lublin, Poland
e-mail: mbarczak@umcs.pl

E. Zięba
SEM Laboratory, Department of Zoology and Ecology, Catholic
University of Lublin, Al. Kraśnicka 102, 20-718 Lublin, Poland

(Cermak et al. 1996; El-Nahhal and El-Ashgar 2007). Modified polysiloxanes have found a wide application in gas chromatography (El-Nasser and Parish 1999) and as active phases of potentiometric sensors (Colilla et al. 2005).

The first family of ordered mesoporous silicas (OMSs) materials called M41S was discovered in 1990 (Yanagisawa et al. 1990; Kresge et al. 1992; Beck et al. 1992); this was followed by discovery of hexagonally arranged and highly ordered SBA-15 materials in 1998 (Zhao et al. 1998a, b; Goltner et al. 1998). OMSs possess many advantages such as easy one-step synthesis, tuneable pores size, thick pore walls, high specific surface area, and good textural properties. Possibility of functionalization of the OMSs makes them very attractive candidates for sensing devices, environmental applications and particularly, for catalytic and adsorption processes (Taguchi and Schüth 2005; Trewyn et al. 2007; Hartmann 2005). Particularly, the amine-functionalized SBA-15 materials have found numerous applications in adsorption of many species including biomolecules and pharmaceuticals (Hartmann 2005; Humphrey et al. 2001; Bui and Choi 2009), as well as heavy metal ions (Liu et al. 2000; Kang et al. 2004; Olkhovik and Jaroniec 2005; Agudo et al. 2009; Barczak et al. 2010). However, there is still little information about application of these materials for removal of noble metals (Kang et al. 2004).

Platinum is one of the most relevant noble metals present in the biosphere, and the recovery of this metal from waters became a very important task, due to its limited world reserves, high cost and wide use in different industries: electrical, petrochemistry, medicine, jewellery, etc. (Jermakowicz-Bartkowiak et al. 2005). On the other hand, there are many problems related to the determination of low concentrations of platinum in the environmental samples where preconcentration step is usually required (Bencs et al. 2003; Zolotov and Kuzmin 1990). The functionalized organosilicas, due to their favoured adsorption characteristics, can be potentially employed for uptake/sorption/recovery of platinum.

In this work the amine-functionalized APX and OMO were synthesized, characterized and compared as sorbents for Pt(II) adsorption. In order to evaluate the possibility of application of synthesized samples for separation and enrichment of Pt(II) from aqueous solutions, the parameters affecting the sorption properties were considered (i.e. pH, contact time, chloride ions concentration and equilibrium Pt(II) ion concentration).

2 Experimental

2.1 Reagents

The following compounds were used: tetraethoxysilane (TEOS, 99 %, ABCR), 3-aminopropyltriethoxysilane

(APTS, 98 %, ABCR), *N*-[3-(trimethoxysilyl)propyl]-ethylenediamine (TMPD, 97 %, ABCR), NH₄F (98 %, POCH), HCl (36 %, POCH), NaOH (POCH), ethanol (EtOH, 99.8 %, POCH), Pluronic P123 (P123, Sigma-Aldrich), potassium tetrachloroplatinate(II) (>99.9 %, Sigma-Aldrich), sodium chloride (POCH), thiourea (POCH), NaCl (POCH), KNO₃ (POCH). All chemicals were used as received, without further purification.

2.2 Synthesis of OMO samples M1–M4

The synthesis of these samples was described by us before (Barczak et al. 2009, 2010). In the model synthesis, 2 g of P123 was dissolved in 60 mL of 2 mol/L HCl and 11 mL of deionized water under vigorous stirring at 40 °C. After 8 h of stirring TEOS was added dropwise to this solution. After 15 min the APTS (samples *M1* and *M2*) or TMPD (samples *M3* and *M4*) was added dropwise. The resulting mixture was stirred at 40 °C for 24 h and aged at 100 °C for next 48 h. The white solid was washed with deionized water, filtered and dried at 70 °C. The template was removed by three-time extraction with the acidified EtOH at 70 °C. The numeration of the samples was as follows: *M0* (TEOS = 20 mmol = 20/0), *M1* (TEOS/APTS = 19/1), *M2* (TEOS/APTS = 18/2), *M3* (TEOS/TMPD = 19/1), *M4* (TEOS/TMPD = 18/2).

2.3 Synthesis of APX samples X1–X4

The syntheses of these samples were similar to those described previously (Zub et al. 2010; Barczak and Borowski 2009). In the model synthesis, a solution of NH₄F was added to the solution of TEOS in 15 mL of EtOH. After 5 min the solution of APTS (samples *X1* and *X2*) or TMPD (samples *X3* and *X4*) in 15 mL of EtOH was added to this mixture. Opalescing gels were formed in a few minutes. After two days, the gel was pounded and dried in vacuum at 30/65/105 °C—2 h at each temperature.

2.4 Instrumental characterization

The CHN elemental analysis was carried out using the Perkin Elmer CHN 2400 analyzer. Powder X-ray diffraction (XRD) patterns were recorded using a Seifert RTG DRON-3 diffractometer (CuK α radiation) with 0.02° size step and 10 s time step covering the range of 0.5° < 2 θ < 5.0° at room temperature. The SEM analysis of randomly selected parts of the surface was performed by means of LEO SEM 1430 VP microscope. The accelerating voltage was set to 20 keV, and the beam current to 80 mA.

Nitrogen adsorption/desorption isotherms were measured at –196 °C using an ASAP-2405 N analyzer. All samples were degassed at 110 °C in vacuum prior to

measurements. BET specific surface areas (S_{BET}) were evaluated in the range of relative pressures p/p_0 of 0.05–0.25 (Brunauer et al. 1938). Total pore volumes (V_p) were calculated by converting the amount adsorbed at $p/p_0 \sim 0.99$ to the volume of liquid adsorbate. Average pore sizes (d_{BJH}) were estimated using the BJH method (Barrett et al. 1951), while pore size distributions (PSD) from the desorption branches of isotherms using the same approach.

XPS spectra were obtained using a Multi-chamber analytical system (Prevac, Poland) with monochromated $K\alpha$ -Al radiation (1486.6 eV) (Gammadata Scienta, Sweden) and an X-ray power of 450 W. The binding energy (BE) scale was referenced against $\text{C1 s} = 284.7$ eV line. The vacuum in the analysis chamber was 8×10^{-9} Pa. The high-resolution scans were performed over the 69–81, 99–110, 192–206, 282–294, 395–407, 527–538 eV ranges for Pt 4f, Si 2p, Cl 2p, C1 s, N1 s and O1 s spectra, respectively.

2.5 Adsorption measurements

The batch mode was used to examine the sorption of Pt(II) ions. In every experiment, 50 mg of adsorbent and 50 mL of platinum solution were stirred at 25 °C. After the adsorption equilibrium had been attained, the solution was separated from the sorbent by centrifugation. The equilibrium adsorption quantity was calculated according to the following formula:

$$a = \frac{(c_i - c) \cdot V}{m}$$

where c_i is the initial Pt(II) concentration (in mg/L), c is the equilibrium Pt(II) concentration (in mg/L), V is the volume of the solution (in L) and m is the mass of the adsorbent (in g). Measurements were carried out using the atomic absorption spectrometer AAS-3 (Carl Zeiss) equipped with a deuterium-lamp background corrector, an EA-3 electrothermal atomizer, and an MPE autosampler. Measurements were performed using the Pt hollow cathode lamp (Varian) at a wavelength of 265.9 nm; 0.2 nm slit width was used. The time–temperature program applied in Pt(II) determination was as follows: drying: 120 °C for 10 s; pyrolysis: 1200 °C for 5 s; atomization: 2600 °C for 2 s. Pure argon

was used as the inert gas with a flow rate of 280 mL/min except the atomization stage.

3 Results

3.1 Synthesis, characterization and efficiency of functionalization

The scheme of the co-condensation of TEOS with functionalized silanes (APTS or TMPD) is presented in Fig. 1. The molar ratios of TEOS/APTS and TEOS/TMPD in the reacting systems were 19:1 and 18:2. Such ratios were selected to achieve the high content of functional groups in the final materials and, in addition, to avoid fast gelation, which is often observed (even in the case of OMO samples) when the relative amount of amine-functionalized silane increases (Dąbrowski et al. 2005). All synthesized samples (OMO and AFX) are non-swelling in common non-aqueous solvents.

The content of nitrogen (and thus amine groups) in the synthesized samples is presented in Table 1. For all APX samples the nitrogen content is around 70–80 % of the theoretical values (calculated from the initial amounts of co-condensing alkoxysilanes). In the case of OMO samples, the nitrogen content is around 50–60 % of the values estimated on the basis of the initial molar composition, indicating less effective incorporation of amine groups than in the case of APX. Apparently, a part of the amine groups is lost during ageing, drying and extraction steps. It can be also seen that in the case of OMO samples there is higher carbon content due to incomplete removal of the template. This is confirmed by the FTIR spectra (not given here) where a group of absorption bands in the region of 2860–3030 cm^{-1} , is attributed to the stretching modes of CH_2 groups of poly(oxyethylene) and poly(oxypropylene) blocks of Pluronic P123 (Barczak et al. 2010).

The nitrogen adsorption–desorption isotherms of the APX and OMO samples are shown in Fig. 2. All the OMO samples exhibit the type IV isotherms according to the IUPAC classification (Rouquerol et al. 1999). The most striking feature is the presence of sharp capillary

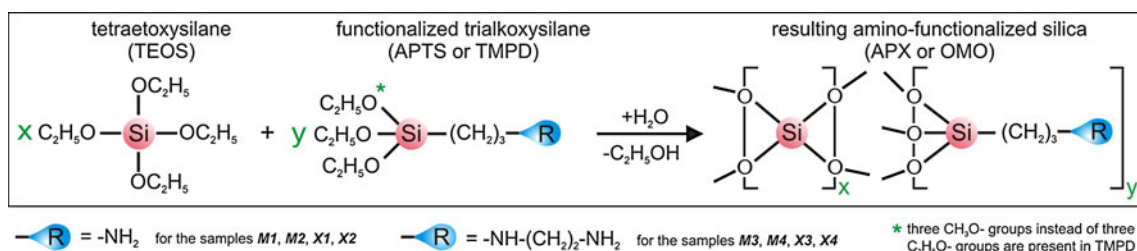


Fig. 1 Scheme of the co-condensation of TEOS with APTS and TMPD

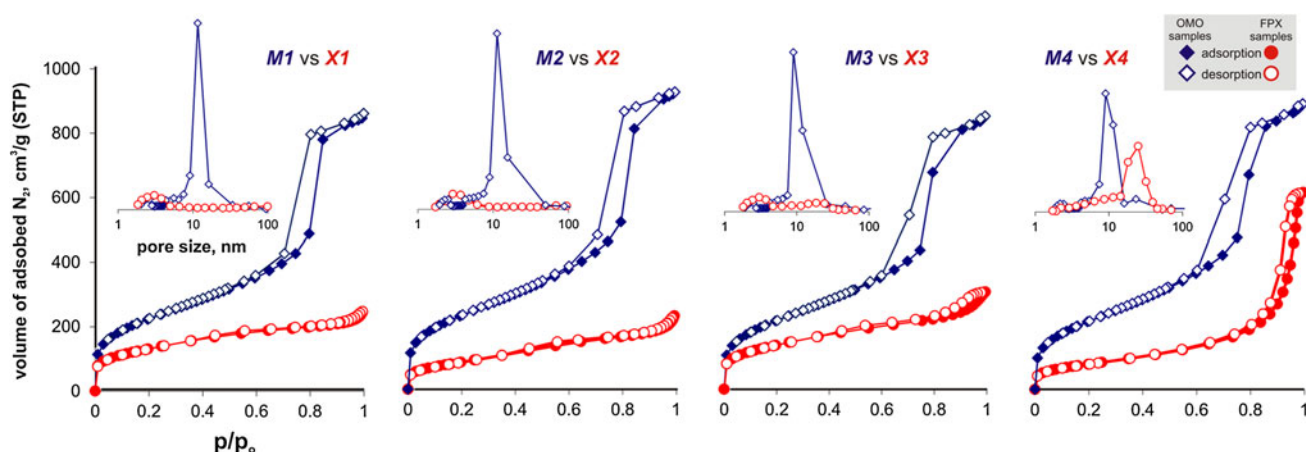
Table 1 Structure-adsorption characteristics of the obtained APX and OMO samples

Sample	Molar composition (mmol)	$S_{\text{BET}}^{\text{a}}$ (m^2/g)	V_{p}^{b} (cm^3)	$d_{\text{BJH}}^{\text{c}}$ (nm)	% N (elemental analysis)	Measured content of amino groups (mmol/g)	Theoretical content of amino groups (mmol/g)
M0	TEOS 20 : 0	789	1.29	5.9	0.00	0.00	0.00
M1	TEOS:APTS 19 : 1	804	1.30	6.8	0.77	0.48	0.80
M2	TEOS: APTS 18 : 2	838	1.43	6.7	1.22	0.76	1.54
M3	TEOS:TMPD 19: 1	808	1.36	6.6	1.21	0.78	1.55
M4	TEOS:TMPD 18 : 2	738	1.30	6.5	2.08	1.34	2.89
X0	TEOS 20 : 0	104	0.06	2.9	0.00	0.00	0.00
X1	TEOS: APTS 19 : 1	467	0.36	3.7	1.00	0.63	0.80
X2	TEOS: APTS 18 : 2	297	0.32	4.4	1.81	1.13	1.54
X3	TEOS:TMPD 19: 1	516	0.48	4.4	1.96	1.26	1.55
X4	TEOS:TMPD 18 : 2	277	0.90	12.1	3.10	2.00	2.89

^a BET specific surface area evaluated in the 0.05–0.25 range of relative pressures

^b Total pore volume (V_{p}) was calculated by converting the amount adsorbed at a relative pressure about 0.99 to the volume of liquid adsorbate

^c Average pore size calculated using the BJH method

**Fig. 2** Nitrogen adsorption/desorption isotherms of the samples studied with corresponding pore size distributions

condensation step, reflecting capillary condensation of adsorbate in the uniform mesopore channels, and evaporation step related to the evacuation of adsorbate from the pores. The isotherms of the samples *M1–M4* exhibit hysteresis loops which is attributed to the presence of mesopores in the material. Those loops can be classified as belonging to the type H1 (Rouquerol et al. 1999). Thus, a framework of these materials has a uniform array of mesopores with the same diameter, which is consistent with the XRD and TEM data (vide infra).

Totally different shapes of the isotherms are observed for the APX samples and their attribution to any IUPAC group is ambiguous. The isotherms of samples *X1* and *X2* exhibit neither capillary condensation, nor hysteresis loop step which means that there are no mesopores, while in the case of *X3* a small hysteresis loop can be observed indicating the presence of some mesopores. In the case of the sample *X4* a steep increase in the adsorption volume of N_2 is observed at p/p_0 close to 0.9. It can be assigned to the presence of intermolecular mesopores between the silica

nanospheres (Sing et al. 1985). The hysteresis loop of *X4* is attributed to the presence of mesopores in the material and is typical of the samples consisting of agglomerates of spheroidal particles of fairly uniform size and array.

The structure-adsorption characteristics are presented in Table 1. The OMO samples have much higher values of the specific surface area (S_{BET}) than corresponding the APX. In the case of OMO, the values of S_{BET} are in the range 740–840 m^2/g while in the case of APX—280–520 m^2/g . The sizes of the ordered mesopores of OMO are in the range 6.5–6.8 nm while for APX—3.7–12.1 nm. Pore volumes are much higher in the case of the OMO samples (1.29–1.43 cm^3/g) when compared with the corresponding APX samples (0.06–0.48 cm^3/g). Only the sample *X4* has a relatively high pore volume (0.90 cm^3), not as high as the corresponding *M4* sample though (1.30 cm^3). The analysis of the values of all parameters confirms deep structural differences between both groups of samples. When comparing the samples within the series, it can be seen that the differences between the values of S_{BET} , V_{p} and d_{BJH} are much lower, larger differences are observed for the APX samples—particularly the sample *X4* differs from the remaining APX samples due to the presence of mesopores.

The pore size distributions of all samples are presented as insets in Fig. 2. For the OMO samples two maxima are present: the first one, a very narrow maximum at ~ 10 nm corresponding to the primary ordered mesopores, and the second one located at ~ 2.5 nm, reflecting the presence of a network of smaller interconnecting pores. For the APX samples *X1*–*X3* wide pore size distributions are observed with one small maximum at ~ 3.5 –4 nm, while for the *X4* sample—at 25, nm indicating totally different porous structure of the latter sample when compared with the other samples from the APX series.

The XRD patterns (not given here) show typical patterns for both series i.e. ordered and amorphous silicas. In the case of OMO samples three well-resolved peaks are usually observed in the range $2\theta \approx 0.8$ – 2° . These peaks can be indexed according to the hexagonal $p6m$ symmetry, indicating a SBA-15 mesostructure: one sharp reflection at $2\theta \approx 0.8$ is indexed as (100) and two minor but distinct reflections at $2\theta \approx 1.4$ and 1.6, are indexed as (110) and (200), respectively. All three signals disappear gradually with the increasing content of amine groups, which means that the ordering of the samples deteriorates. In the case of APX no signals in the low-angle range are observed demonstrating the lack of any type of ordering and amorphous character of the APX samples.

The SEM micrographs of the samples *M1*, *X1* and *X4* are presented in Fig. 3. All the OMO samples are composed of irregular “needle-like” particles having worm-like structure, i.e. parallelly oriented hexagonal motifs. The

APX samples are composed of aggregated spherical particles. In the case of the sample *X4* empty spaces between the aggregates make this sample less compact, when compared to the other samples from the APX series.

3.2 Sorption studies

First, the effect of pH on Pt(II) adsorption onto the synthesized materials was studied. The series of solutions of the same platinum concentration were prepared and proper initial pH (pH_{in}) values were set up by adding the hydrochloric acid or sodium hydroxide. Then the Pt(II) sorption measurements were performed for each solution. In the case of APTS-functionalized samples, the highest adsorption capacity is obtained for the equilibrium pH (pH_{eq}) of 2.5 and 3.3 for *M2* and *X2*, respectively (Fig. 4). However, the shapes of both curves are different. In the case of sample *M2* the changes of the Pt(II) uptake are strongly pH-dependent, showing a narrow maximum. In contrast, *X2* curve exhibits a wide maximum covering the range ~ 1.8 –4.4. It is worth noting that in the case of sample *M2* insignificant differences in pH_{eq} are observed for pH_{in} between 3.5 and 7. It means that in this range a buffering effect occurs. For the sample *X2* analogous phenomenon is observed for $\text{pH}_{\text{eq}} \approx 5$.

The effect of pH on Pt(II) uptake by the TMPD-functionalized samples is shown in Fig. 4. The maximum uptake for *M4* is achieved at $\text{pH}_{\text{eq}} \approx 2.5$, and for *X4* the plateau is observed in the range of $\text{pH}_{\text{eq}} \sim 0.8$ –5.5 and is slightly pH-dependent for both materials. Outside this range a significant decrease in the adsorbed Pt(II) species is observed. Similarly to the materials functionalized by APTS, the buffering effect in the range of $\text{pH}_{\text{eq}} \sim 3.5$ for *M4* and ~ 5.5 for *X4*, is observed.

The effect of time on adsorption of Pt(II) ions onto the synthesized materials was studied and is presented in Fig. 5. For the APTS-functionalized samples the rate of the Pt(II) adsorption is significantly slower for APXs than for OMOs. The adsorption equilibrium for the samples *M1* and *M2* is achieved after 5 and 10 h, respectively, whereas for the samples *X1* and *X2* after 72 and 20 h, respectively. For *X3* only a 45 min interval is required for reaching the equilibrium, and 18 h are necessary for *M3*. Very slow kinetics for *X1* and *X2* compared to *M1* and *M2* (cf. Fig. 5) is probably associated with a considerable content of the amine groups localized in the micropores for APX materials. In the case of OMO samples, the existing micropores follow from the penetration of the silica framework by hydrophilic parts of P123, thus there should be no considerable number of nitrogen centres located in the micropores. Moreover, in the case of *X1* and *X2* samples there are no mesopores facilitating the transport of Pt(II) ions while in the case of all OMO samples mesopores are

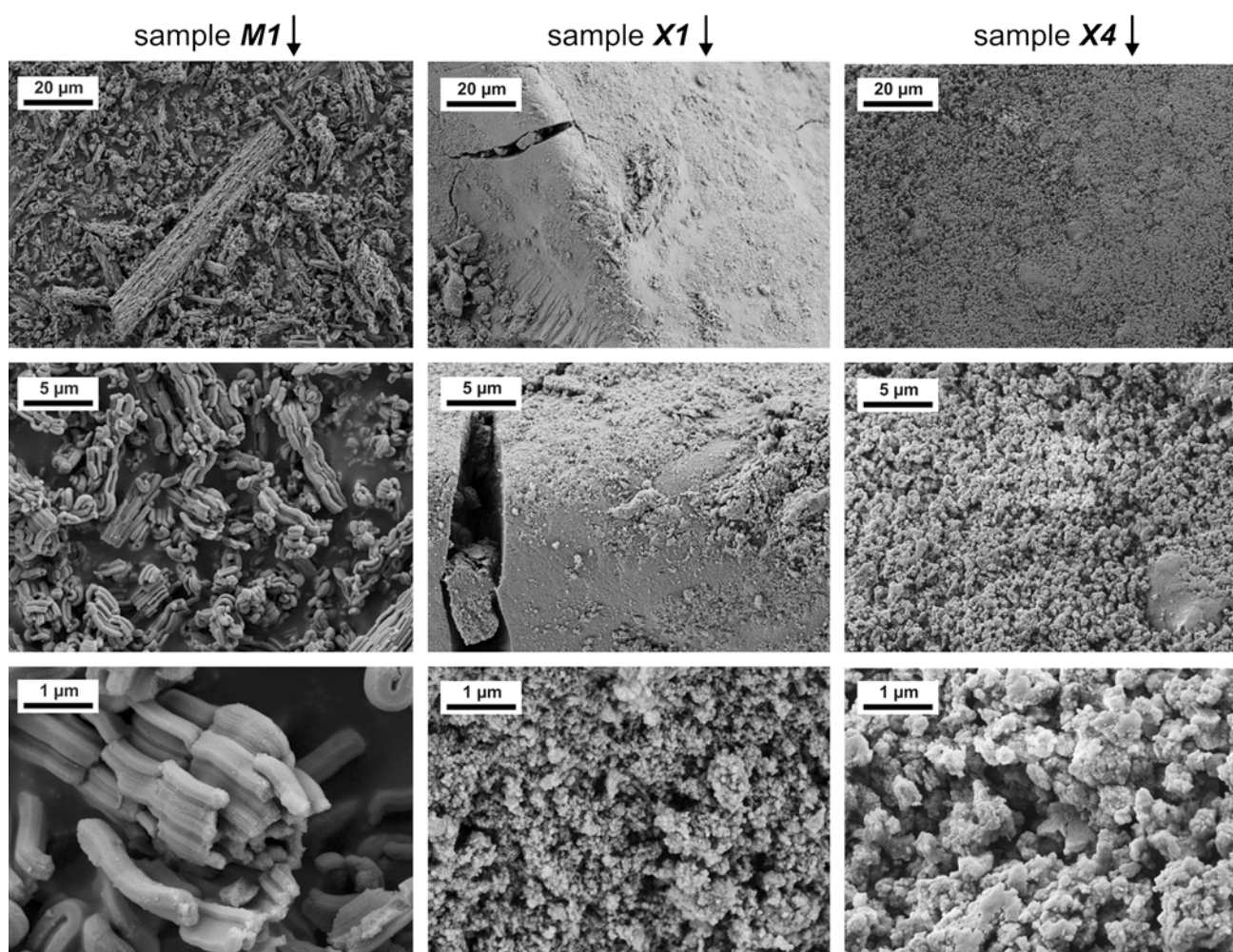


Fig. 3 SEM photographs of the samples *M1*, *X1*, and *X4*

predominant in the porous structure. As a result, there is a slow transport rate of Pt(II) ions to the micropores of the adsorbent. In the case of *X3* and *X4* the amount of mesopores is higher than for *X1* and *X2* (cf. Fig. 2) Therefore the diffusion into the micropores is facilitated and the adsorption kinetics is much faster. However, despite the relevant mesoporosity in the case of *X4* sample as compared with *X3*, the time needed for reaching equilibrium state is comparable. This suggests that the chemical reactions occurring during the adsorption process are relatively slow constituting the limiting factor for the TMPD-functionalized APX samples.

In order to determine the selectivity of the Pt(II) sorption from aqueous solutions onto the amine-functionalized silicas, the effect of chloride ions on Pt(II) adsorption ability was studied in detail. In Fig. 6 the effect of chlorides on the adsorption of Pt(II) is presented. In the case of *M2*, *M4* and *X2* the presence of chlorides concentration higher than 0.01 mol/L causes drastic decrease of the adsorption by about 80–90 %. In turn, in the case of *X4* the

presence of chlorides at the concentration below 0.5 mol/L does not cause the decrease of Pt(II) adsorption. For higher concentrations of chlorides the adsorption of Pt(II) on *X4* decreases almost proportionally to the chlorides content up to 70 % for 3 mol/L chlorides solution. Different behaviour of *X4* seems to be the effect of higher adsorption pH compared to *M2*, *M4* and *X2*. The content of amine groups for *X4* is the highest comparing with other studied sorbents. Therefore, it appears that pH in the vicinity of sorbent surface is higher than in the bulk solution and as a result, the hydrolysis of PtCl_4^{2-} complex to more stable aqueous and hydroxy platinum complexes takes place. For the higher pH value deprotonation of surface amine groups facilitates the adsorption of platinum complexes.

The adsorption ability of APTS-functionalized OMO and APX has been determined by measuring the Pt(II) uptake from its aqueous solutions. The adsorption isotherms are presented in Fig. 7. As it can be noticed for the silicas functionalized by APTS, the adsorbed amount obtained for the OMO samples *M1* and *M2* is about 1.7 times higher than

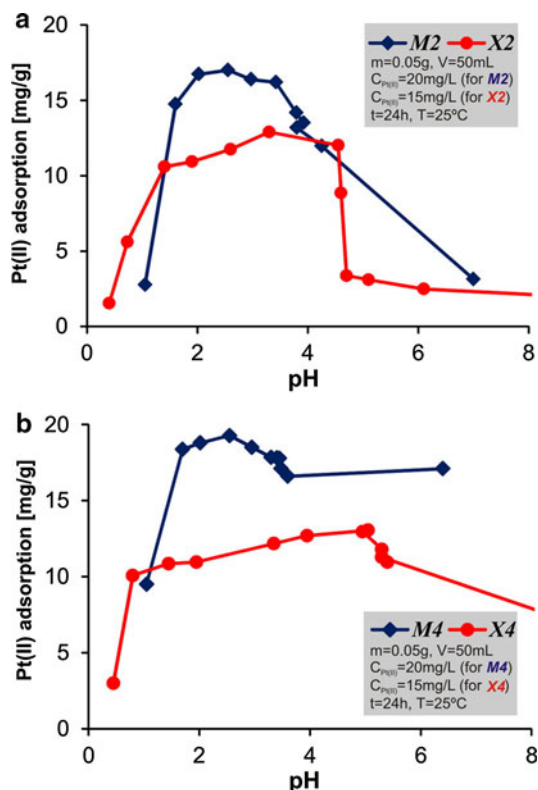


Fig. 4 The pH influence on Pt(II) adsorption for the samples *M2/X2* and *M4/X4*

the corresponding values for the APX samples *X1* and *X2*. However, the amounts of nitrogen in the *X1* and *X2* samples are significantly higher than for *M1* and *M2*, respectively, which suggests that the adsorption of Pt(II) ions in the amorphous APTS-functionalized samples is hindered due to limited adsorbate diffusion into the micropores.

For the pure silica samples *M0* and *X0* no Pt(II) uptake was observed testifying the fact that the composition of the

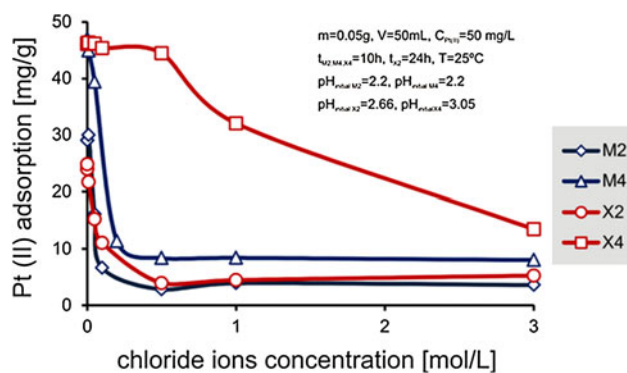
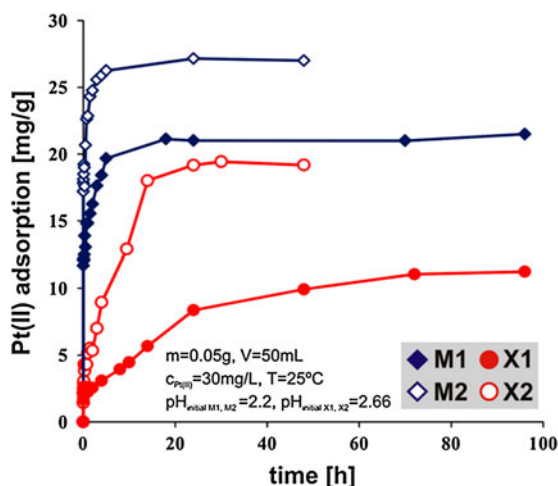


Fig. 6 The influence of chloride ions on Pt(II) adsorption

surface layer is the factor influencing the adsorption properties of the studied systems. The measured values of static sorption capacities (SSC) are 32, 20, 65 and 36 $\text{mg}_{\text{Pt(II)}}/\text{g}$ for *M1*, *X1*, *M2* and *X2*, respectively. For the TMPD-functionalized silicas the opposite trend is observed, i.e., higher values of SSC are obtained for the APX than for OMO samples. The measured values of static sorption capacities (SSC) are 50, 87, 102 and 139 $\text{mg}_{\text{Pt(II)}}/\text{g}$ for *M3*, *X3*, *M4* and *X4*, respectively. Moreover, in the case of the TMPD-functionalized silicas, the adsorption capacities are correlated with the nitrogen content in these sorbents. High SSC values and relatively fast kinetics observed for *X3* and *X4* suggest that due to the presence of numerous mesopores in the structure of these samples the transport of Pt(II) ions to the adsorption centres localized in micropores is easier than in the case of the samples *X1* and *X2*. Moreover, a fraction of amine groups is probably inaccessible for Pt(II) ions in the case of the latter one.

The isotherms presented in Fig. 7 exhibit the Langmuirian behaviour and may be described by the Langmuir–Freundlich equation given as:

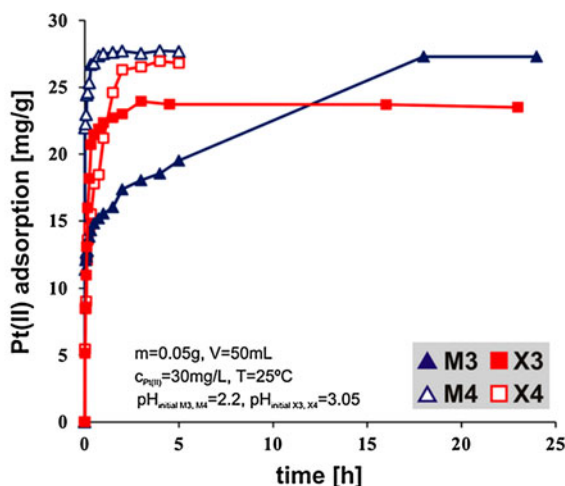


Fig. 5 Adsorption kinetics curves for the samples studied

$$a = a_m \frac{(Kc)^n}{1 + (Kc)^n} \quad (1)$$

where, a is the amount of adsorbed platinum at the adsorption equilibrium state [mg/g], a_m is the maximum adsorption capacity [mg/g], K is the Langmuir constant, c is the equilibrium concentration of Pt(II) [mg/L]. The parameter n is the factor characterizing the quasi-Gaussian energetic heterogeneity of the adsorption system. As the value of this parameter decreases, the energetic heterogeneity of the adsorbent surface increases. In the case when $n \rightarrow 0$ there is high heterogeneity. For $n \rightarrow 1$, equation (1) simplifies to the classical Langmuir adsorption isotherm equation describing the homogeneous adsorbents. On the other hand, in the case of very small equilibrium concentrations, the factor $(Kc)^n$ in equation (1) is much lower than 1, so that equation (1) reduces to the form:

$$a = a_m (Kc)^n, \quad (2)$$

which is known as the Freundlich isotherm equation, very often used for explanation of adsorption data because of its simplicity (Jaroniec 1983). The linear form of the Freundlich equation can be expressed as:

$$\ln a = \ln(a_m K) + n \ln c, \quad (3)$$

where the Langmuir constant K is related to the Freundlich constant C_0 by the relation:

$$K = (C_0)^{-n} \quad (4)$$

which, when inserted into equation (3), leads to the following equation:

$$\ln a = \ln[a_m (C_0)^{-n}] + n \ln c \quad (5)$$

Equation 5 was used to calculate the values of K , C_0 , a_m , n , and the correlation coefficients R^2 which are shown in

Table 2. The isotherms presented in Fig. 7 show that the adsorption of Pt(II) ions satisfies well Eq. 5 (i.e. the Freundlich adsorption isotherm). Comparing the values of parameter n some additional relations can be found. For the ordered silica the decrease in the n values along with the nitrogen content increase is observed. It means that energetic heterogeneity of the functionalized ordered silica increases along with the increase of the nitrogen content. For the disordered functionalized silica, the parameter n shows an opposite tendency, along with the increase of the nitrogen content the increase of the n values can be noted. Energetic heterogeneity decreases along with the increase of the nitrogen content, and for X3 and X4 these materials become energetically homogeneous for the studied adsorption system.

In Table 3 the static sorption capacities of the samples studied here are compared with other studies for Pt(II) sorption found in the literature (Vassileva et al. 2008; Cox et al. 2005). The materials studied here have a superior properties and the values of static sorption capacity for Pt(II) ions are the highest when compared with those presented in the former works (Yin et al. 2010; Vassileva et al. 2008; Cox et al. 2005).

In order to explain the mechanism of Pt(II) ions adsorption onto the amine-functionalized silicas and their chemical behavior on their surfaces, the XPS studies were undertaken. In Fig. 8a the XPS spectrum of the Pt 4f region for the Pt loaded TMPD-functionalized OMO, being a cut of the full spectrum is shown. For M4 platinum species are characterized by two peaks in the line with the Pt 4f7/2 and Pt 4f5/2 transitions. This doublet with the peaks (4f7/2 and 4f5/2) at 73.2 and 76.5 eV is assigned to Pt(II) (Drelinkiewicz et al. 2009). Therefore, the platinum in the second oxidation state is the dominant form of platinum species present on the TMPD-functionalized surface.

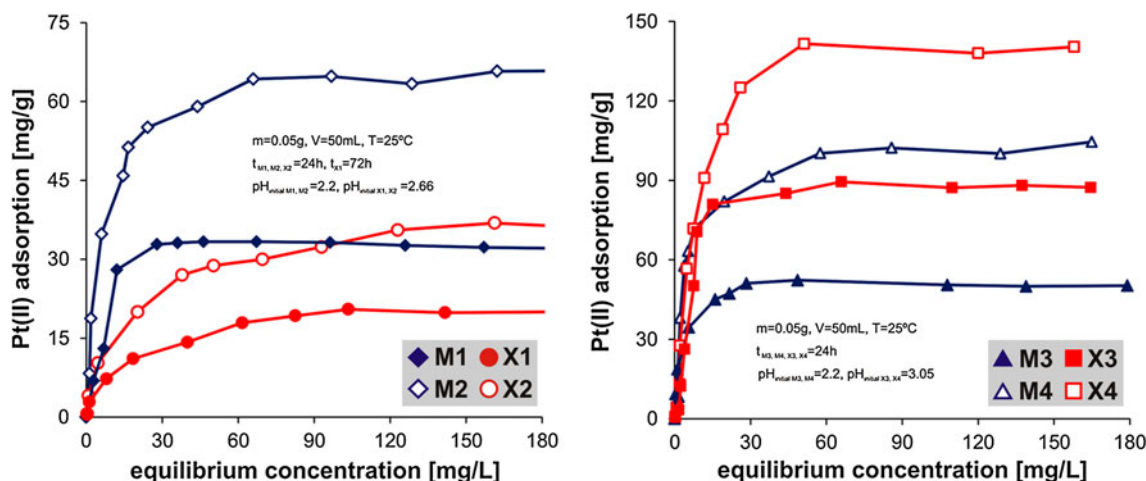


Fig. 7 Adsorption isotherms of Pt(II) for the samples studied

Table 2 Langmuir-Freundlich parameters for adsorption of Pt(II) ions on the samples studied

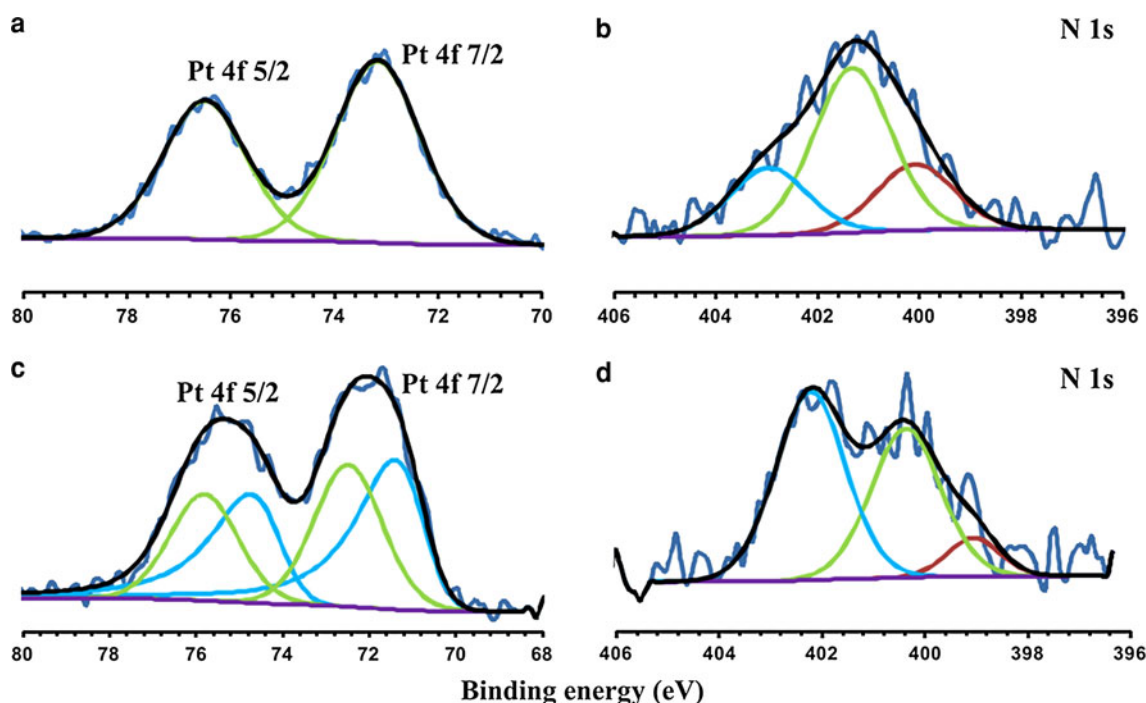
Sample	a_m (mg/g)	n	K	c_o (mg/L)	R^2
<i>M1</i>	32	0.73	0.09	26.48	0.923
<i>X1</i>	20	0.44	0.14	85.83	0.993
<i>M2</i>	65	0.31	0.29	59.02	0.913
<i>X2</i>	36	0.42	0.14	107.36	0.974
<i>M3</i>	50	0.36	0.31	26.08	0.950
<i>X3</i>	87	1.01	0.07	13.37	0.964
<i>M4</i>	102	0.20	0.52	34.43	0.957
<i>X4</i>	139	1.03	0.04	18.50	0.955

Additionally, it was stated that for unloaded *M4* the XPS spectra of N1s region are characterized by two peaks at 399.1 and 401.4 eV, which corresponds to $-\text{NH}-$ and $-\text{NH}_2$ groups (Li et al. 2009). On the other hand, for Pt loaded *M4* (Fig. 8b) triplet of N1s is observed with the peaks at 400.1,

401.3 and 402.9 eV. The appearance of the third peak with a slight intensity at 402.9 may be explained by oxidation mechanism of $-\text{NH}-$ groups to $-\text{N}^+=\text{O}$. It worth to emphasizing that partial transformation of Pt(II) to Pt(IV) takes place in the acidic liquid medium (Nischwitz et al. 2003). It means that part of Pt(II) in a bulk solution could be oxidized to Pt(IV) during the adsorption process (24 h). Simultaneously, Pt(IV) ions were reduced to Pt(II) onto the TMPD-functionalized OMO surface. In the case of Pt loaded APTS-functionalized OMO, the two doublets with the peaks (4f7/2) at 72.5 and 71.4 and (4f5/2) at 75.8 and 74.7 eV, respectively, are observed on the XPS spectra of the Pt 4f region (Fig. 8c). The first pair of peaks corresponds to the Pt(II) presence, whereas the second doublet proves the presence of metallic Pt. Therefore it is probable that in the case of *M2* the partial reduction of Pt(II) to Pt(0) takes place. In the case of Pt loaded *M2* triplet for N1s region with the peaks at 399.1, 400.3 and 402.2 eV is also observed

Table 3 Comparison of static sorption capacities with regards to Pt(II) species found in the literature

Sorbent	pH	SSC (mg/g)	Ref.
Silica gel microspheres encapsulated by imidazole functionalized polystyrene	5.0	68	(Yin et al. 2010)
Thiouracil modified activated carbon	1.0	48	(Vassileva et al. 2008)
Carbon from flax shive	6.5	90	(Cox et al. 2005)
SBA-15 organosilica functionalized with amine groups	2.2	102	This study
Amorphous silica xerogels functionalized with amine groups	2.2	139	This study

**Fig. 8** XPS spectrum of sample *M4* and *M2*: **a** Pt 4f region of Pt loaded *M4*, **b** N 1s region of Pt loaded *M4*, **c** Pt 4f region of Pt loaded *M2*, and **d** N 1s region of Pt loaded *M2*

(Fig. 8d). The first two peaks correspond to $-\text{NH}_2$ group in the presence of $[\text{PtCl}_4]^{2-}$, forming surface complex. Whereas the peak at 402.2 eV corresponds to the unprotonated $-\text{N}=\text{O}$ group, coming from oxidation of amine groups. The mechanism of Pt(II) sorption proposed above should be confirmed by another independent method (e.g. Mössbauer spectroscopy) to exclude the influence of X-ray beam on the platinum species during the XPS measurements.

High adsorption capacities of the studied organosilicas create opportunity for their use in the platinum preconcentration and separation from the environmental samples. In order to find how many sorption/desorption cycles can be performed with the prepared sorbents desorption studies were carried out. As the desorption medium HNO_3 , HCl and thiourea in 1.0 mol/L HCl solutions with respect to their concentrations were proposed.

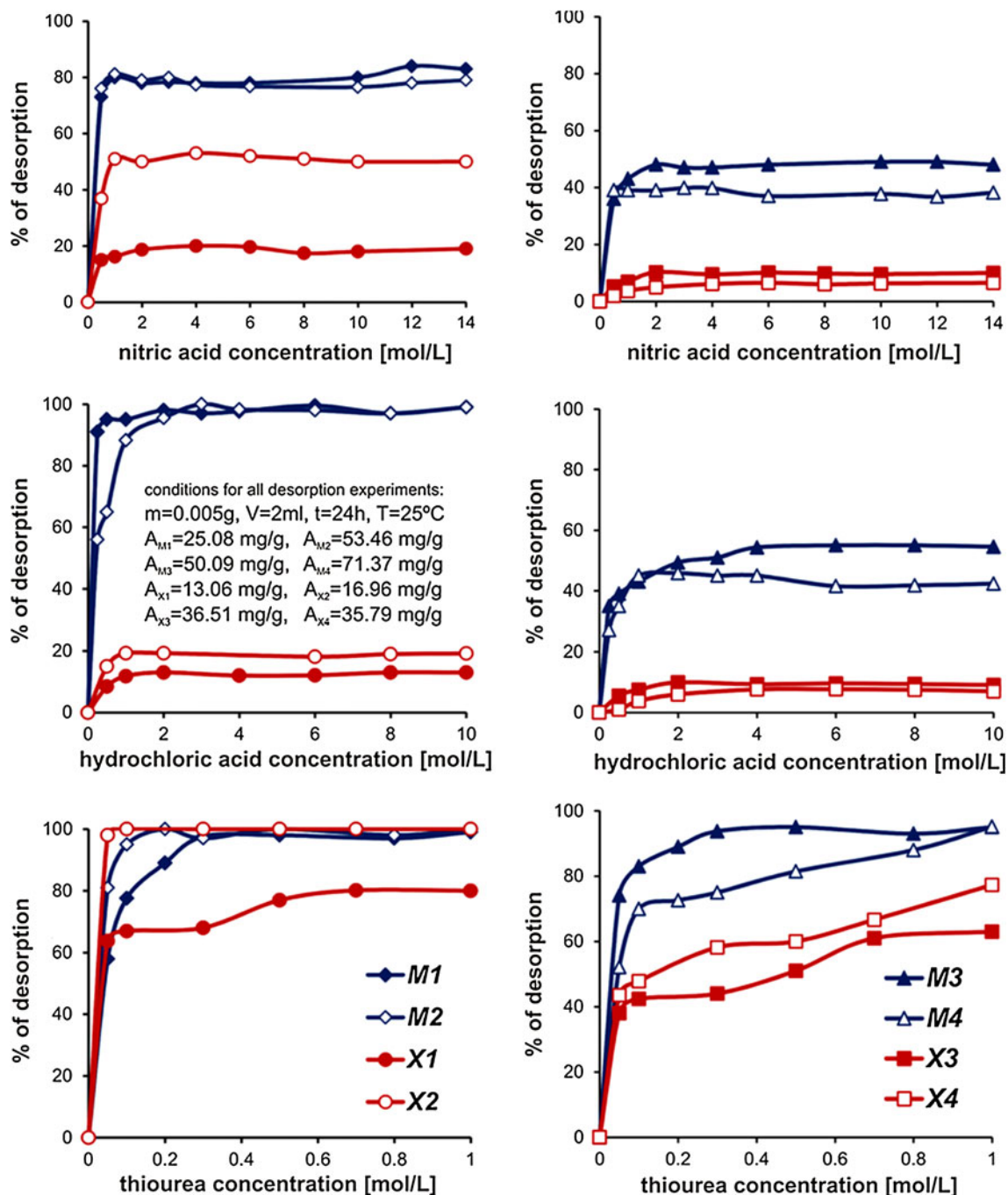


Fig. 9 Desorption of platinum species from the samples *M1–M4* and *X1–X4* by nitric acid, hydrochloric acid and thiourea solutions

The application of HNO_3 as the desorption medium was chosen due to the fact that the nitrate does not form a stable complex with Pt(II) and Pt(IV) ions, so its desorption activity is connected only with the competition effect to adsorption centres. In the case of HCl beyond the competition effect, chlorides can replace OH^- groups in the coordination zone of platinum ions. Whereas thiourea forms a very stable complex with platinum ions so it can compete with $-\text{NH}_2$ surface groups.

The desorption study has been presented in Fig. 9. The application of HNO_3 causes a partial desorption of platinum species from OMO, whereas for APX especially for X3 and X4 desorption was negligible. In the case of HCl, the application of 2 mol/L solution cause the total desorption of platinum species from M1 and M2. While for APX the desorption was lower and does not exceed 10 %. When thiourea in 1.0 M HCl was applied as the desorption medium, the total desorption of platinum species from M1, M2, M3, M4 and X2 materials was reached. Only for X1, X3 and X4 the platinum species desorption was not quantitative. To summarize, the application of OMOs modified by APTS and TMPD for the Pt(II) ions preconcentration and desorption by thiourea in 1 mol/L HCl creates the possibility of multiple use of sorbents.

4 Conclusions

Amorphous polysiloxane xerogels (APX) and ordered mesoporous organosilicas (OMO) functionalized with the amine groups have been synthesized by co-condensation of proper monomers. The OMOs samples have well-ordered porous structure, with the values of specific surface areas in the range 740–840 m^2/g , which are noticeably higher than the corresponding values for the APX samples (280–520 m^2/g). The porous structure for both series of the samples is totally different. Both series of silicas have high contents of amine groups: 0.5–1.3 mmol/g in the case of OMO and 0.6–2.0 mmol/g in the case of APX. This means 70–80 % incorporation efficiency of the amine groups for APX and 50–60 % for the OMO samples was achieved.

Both series contain different fractions of mesopores and micropores which play a crucial role in the case of Pt(II) adsorption kinetics. The presence of micropores causes slow transport of Pt(II) ions to the adsorption species and makes a fraction of the amine groups inaccessible to these ions. The adsorption of Pt(II) ions is strongly pH-dependent and the values of the maximum sorption capacities calculated from the Langmuir–Freundlich equation are in the range 32–102 $\text{mg}_{\text{Pt(II)}/\text{g}}$ and 20–139 $\text{mg}_{\text{Pt(II)}/\text{g}}$ for the OMO and APX series, respectively. Thus the obtained silica adsorbents show strong affinity for Pt(II), and the proper choice of silica sorbent

(e.g. OMO vs. APX) plays a very important role in the case of the Pt(II) adsorption.

Acknowledgments Mariusz Barczak and Andrzej Dąbrowski acknowledge the Polish Ministry of Science and Higher Education for supporting the research under Grant No. N N204 111135. Dr Piotr Borowski is also acknowledged for his help with the preparation of the manuscript.

Open Access This article is distributed under the terms of the Creative Commons Attribution License which permits any use, distribution, and reproduction in any medium, provided the original author(s) and the source are credited.

References

- Aguado, J., Arsuaga, J.M., Arencibia, A., Lindo, M., Gascon, V.: Aqueous heavy metals removal by adsorption on amine-functionalized mesoporous silica. *J. Hazard. Mat.* **163**, 213–221 (2009)
- Avnir, D., Klein, L.C., Levy, D., Schubert, U., Wójcik, A.B.: Organosilica sol-gel materials. In: Rappoport, Z., Apeloig, Y. (eds.) *The Chemistry of Organic Silicon Compounds* vol 2, p. 2317. Wiley, New York (1998)
- Barczak, M., Pikus, S., Skrzydło-Radomańska, B., Dąbrowski, A.: Synthesis, structure and adsorption properties of nanoporous SBA-15 materials with framework and surface functionalities. *Adsorption* **15**, 278–286 (2009a)
- Barczak, M., Borowski, P., Dąbrowski, A.: Structure-adsorption properties of ethylene bridged polysilsesquioxanes functionalized with different groups. *Colloids Surf. A* **347**, 114–120 (2009b)
- Barczak, M., Skwarek, E., Janusz, W., Dąbrowski, A., Pikus, S.: Functionalized SBA15 organosilicas as sorbents of zinc(II) ions. *Appl. Surf. Sci.* **256**, 5370–5375 (2010a)
- Barczak, M., Dąbrowski, A., Pikus, S., Ryczkowski, J., Borowski, P., Kozak, M.: Studies of the structure and chemistry of SBA-15 organosilicas functionalized with amine, thiol, vinyl and phenyl groups. *Adsorption* **16**, 457–463 (2010b)
- Barrett, E.P., Joyner, L.G., Halenda, P.P.: The determination of pore volume and area distributions in porous substances. I. Computations from nitrogen isotherms. *J. Am. Chem. Soc.* **73**, 373–380 (1951)
- Beck, J.S., Vartuli, J.C., Roth, W.J., Leonowicz, M.E., Kresge, C.T., Schmitt, K.D., Chu, C.T.-W., Olsen, D.H., Sheppard, E.W., McCullen, S.B., Higgins, J.B., Schlenker, J.L.: A new family of mesoporous molecular sieves prepared with liquid crystal templates. *J. Am. Chem. Soc.* **114**, 10834–10843 (1992)
- Bencs, L., Ravindra, K., van Grieken, R.: Methods for the determination of platinum group elements originating from the abrasion of automotive catalytic converters. *Spectrochim. Acta B* **58**, 1723–1755 (2003)
- Brinker, C.J., Scherer, G.W.: *Sol-gel science*. Academic, Nowy Jork (1990)
- Brunauer, J.S., Emmet, P.H., Teller, E.: Adsorption of gases in multimolecular layers. *J. Am. Chem. Soc.* **60**, 309–319 (1938)
- Bui, T.X., Choi, H.: Adsorptive removal of selected pharmaceuticals by mesoporous silics SBA-15. *J. Hazard. Mat.* **168**, 602–608 (2009)
- Cermak, J., Kvalcova, M., Blechta, V., Capka, M., Bastl, Z.: Hydrogenation catalytic activity of substituted cyclopentadienyl titanium complexes anchored on polysiloxanes prepared by a sol-gel procedure. *J. Organomet. Chem.* **509**, 77–84 (1996)

- Colilla, M., Darder, M., Aranda, P., Ruiz-Hitzky, E.: Amino-polysiloxane hybrid materials as carbon composite electrodes for potentiometric detection of anions. *J. Mater. Chem.* **15**, 3844–3851 (2005)
- Collinson, M.M.: Critical sol-gel strategies for the preparation of selective materials for chemical analysis. *Rev. Anal. Chem.* **29**, 289–311 (1999)
- Cox, M., Pichugin, A., El-Shafey, E.I., Appleton, Q.: Sorption of precious metals onto chemically prepared carbon from flax shive. *Hydrometallurgy* **78**, 137–144 (2005)
- Dąbrowski, A., Barczak, M., Stolyarchuk (Shvaykovska), N.V., Melnyk, I.V., Zub, Y.L.: Bridged polysiloxane xerogels functionalized by amine- and thiol- groups: synthesis, structure, adsorption properties. *Adsorption* **11**, 501–517 (2005)
- Dąbrowski, A., Barczak, M., Dudarko, O.A., Zub, Y.L.: Preparation and characterization of polysiloxane xerogels having covalently attached phosphonic groups. *Pol. J. Chem.* **81**, 475–483 (2007)
- Drelinkiewicz, A., Sobczak, J.W., Sobczak, E., Krawczyk, M., Zieba, A., Waksmundzka-Góra, A.: Physicochemical and catalytic properties of Pt-poly(4-vinylpyridine) composites. *Mater. Chem. Phys.* **114**, 763–773 (2009)
- El-Nahhal, I.M., El-Ashgar, N.M.: A review on polysiloxane-immobilized ligand systems; synthesis, characterization and applications. *J. Organomet. Chem.* **692**, 2861 (2007)
- El-Nasser, A.A., Parish, R.V.: Solid polysiloxane ligands containing glycine- or iminodiacetate- groups: synthesis and application to binding and separation of metal ions. *J. Chem. Soc. Dalton Trans.* **19**, 3463–3466 (1999)
- Feng, X., Fryxell, G.E., Wang, L.-Q., Kim, A.Y., Liu, J., Kemner, K.M.: Functionalized monolayers on ordered mesoporous supports. *Science* **276**, 923–926 (1997)
- Ferey, G.: Hybrid porous solids: past, present, future. *Chem. Soc. Rev.* **37**, 191–214 (2008)
- Goltner, C.G., Henke, S., Weissenberger, M.C., Antonietti, M.: Mesoporous silica from lyotropic liquid crystal polymer templates. *Chem. Int. Ed.* **37**, 613–616 (1998)
- Hartmann, M.: Ordered mesoporous materials for bioadsorption and biocatalysis. *Chem. Mater.* **17**, 4577–4593 (2005)
- Humphrey, H.H.P., Botting, C.H., Botting, N.P., Wright, P.A.: *Phys. Chem. Chem. Phys.* **3**, 2983–2985 (2001)
- Jaroniec, M.: Physical adsorption on heterogeneous solids. *Adv. Coll. Inter. Sci.* **18**, 149–225 (1983)
- Jermakowicz-Bartkowiak, D., Kolarz, B.N., Serwin, A.: Sorption of precious metals from acid solutions by functionalised vinylbenzyl chloride-acrylonitrile-divinylbenzene copolymers bearing amino and guanidine ligands. *React. Funct. Polym.* **65**, 135–142 (2005)
- Kang, T., Park, Y., Yi, J.: Highly selective adsorption of Pt^{2+} and Pd^{2+} using thiol-functionalized mesoporous silica. *Ind. Eng. Chem. Res.* **43**, 1478–1484 (2004a)
- Kang, T., Park, Y., Choi, K., Lee, J.S., Yi, J.: Ordered mesoporous silica (SBA-15) derivatized with imidazole-containing functionalizes as a selective adsorbent of precious metal ions. *J. Mater. Chem.* **14**, 1043–1049 (2004b)
- Kickelbick, G.: Introduction to hybrid materials. In: Kickelbick, G. (ed.) *Hybrid Materials*. Wiley-VCH Verlag GmbH & Co. KGaA, Weinheim (2007)
- Kresge, C.T., Leonowicz, M.E., Roth, W.J., Vartuli, J.C., Beck, J.S.: Ordered mesoporous molecular sieves synthesized by a liquid-crystal template mechanism. *Nature* **359**, 710–712 (1992)
- Li, X.G., Ma, X.L., Sun, J., Huang, M.R.: Powerful reactive sorption of silver(I) and mercury(II) onto poly(o-phenylenediamine) microparticles. *Langmuir* **25**, 1675–1684 (2009)
- Liu, A.M., Hidajat, K., Kawi, S., Zhao, D.Y.: A new class of hybrid mesoporous materials with functionalized organic monolayers for selective adsorption of heavy metal ions. *Chem. Commun.* **13**, 1145–1146 (2000)
- Loy, D.A., Jamison, G.M., Baugher, B.M., Myers, S.A., Assink, R.A., Shea, K.J.: Sol-gel synthesis of hybrid organic-inorganic materials. hexylene- and phenylene-bridged polysiloxanes. *Chem. Mater.* **8**, 656–663 (1996)
- Nischwitz, V., Michalke, B., Kettrup, A.: Speciation of Pt(II) and Pt(IV) in spiked extracts from road dust using on-line liquid chromatography-inductively coupled plasma mass spectrometry. *J. Chromatogr. A* **1016**, 223–234 (2003)
- Olkhoviyk, O., Jaroniec, M.: Ordered mesoporous silicas with 2,5-dimercapto-1,3,4-thiadiazole ligand: high capacity adsorbents for mercury ions. *Adsorption* **11**, 205–214 (2005)
- Rouquerol, F., Rouquerol, J., Sing, K.: *Adsorption by Powders and Porous Solids. Principles, Methodology and Application*, pp. 18–20. Academic Press, London (1999)
- Sakka, S. (ed.): *Handbook of Sol-Gel Science and Technology: Processing, Characterization, and Applications*. Kluwer, Dordrecht (2005)
- Shea, K.J., Moreau, J., Loy, D.A., Corriu, R.J.P., Boury, B.: Bridged polysiloxanes. Molecular-engineering nanostructured hybrid organic-inorganic materials. In: Gomez-Romero, P., Sanchez, C. (eds.) *Functional Hybrid Materials*, pp. 50–85. Wiley-VCH, Weinheim (2004)
- Sing, K.S., Everett, D.H., Haul, R.A.W., Moscou, L., Pierotti, R.A., Rouquerol, J., Siemieniowska, T.: Reporting physisorption data for gas/solid systems with special reference to the determination of surface area and porosity. *Pure Appl. Chem.* **57**, 603–619 (1985)
- Slinyakova, I.B., Denisova, T.I.: *Kremniorganicheskie adsorbenty. Poluchenie, svoystva, primeneniye (Organosilicon Adsorbents: Synthesis, Properties, Applications)*. Naukova Dumka, Kiev (1988)
- Taguchi, A., Schüth, F.: Ordered mesoporous materials in catalysis. *Microporous Mesoporous Mater.* **77**, 1–45 (2005)
- Trewyn, B.G., Giri, S., Slowing, I.I., Lin, V.S.-Y.: Mesoporous silica nanoparticle based controlled release, drug delivery, and biosensor systems. *Chem. Commun.* **31**, 3236–3245 (2007)
- Vassileva, P., Tzvetkova, P., Lakov, L., Peshev, O.: Thiouracil modified activated carbon as a sorbent for some precious and heavy metal ions. *J. Porous Mater.* **15**, 593–599 (2008)
- Yanagisawa, T., Shimizu, T., Kuroda, K., Kato, C.: The preparation of alkyltrimethylammonium-kanemite complexes and their conversion to microporous materials. *Bull. Chem. Soc. Jpn.* **63**, 988–992 (1990)
- Yin, P., Xu, Q., Qu, R., Zhao, G., Sun, Y.: Adsorption of transition metal ions from aqueous solutions onto a novel silica gel matrix inorganic-organic composite material. *J. Hazard. Mater.* **173**, 710–716 (2010)
- Zhao, D.Y., Feng, J.L., Huo, Q.S., Melosh, N., Fredrickson, G.H., Chmelka, B.F., Stucky, G.D.: Triblock copolymer syntheses of mesoporous silica with periodic 50 to 300 angstrom pores. *Science* **279**, 548–552 (1998a)
- Zhao, D.Y., Huo, Q.S., Feng, J.L., Chmelka, B.F., Stucky, G.D.: Nonionic triblock and star diblock copolymer and oligomeric surfactant syntheses of highly ordered, hydrothermally stable, mesoporous silica structures. *J. Am. Chem. Soc.* **120**, 6024–6036 (1998b)
- Zolotov, Y.A., Kuzmin, N.M.: *Preconcentration of Trace Elements*. Elsevier, Amsterdam (1990)
- Zub, Y.L., Stolyarchuk, N.V., Barczak, M., Dąbrowski, A.: Surface heterogeneity of polysiloxane xerogels functionalized by 3-aminopropyl groups. *Appl. Surf. Sci.* **256**, 5361–5364 (2010)